Frontiers of micro and nanomechanics of materials: Soft or amorphous matter, surface effects

Determinations of both length scale and surface elastic parameters for fcc metals

Jingru Song, Jianyun Liu, Hansong Ma, Lihong Liang, Yuegaung Wei *

State-Key Laboratory of Nonlinear Mechanics, Institute of Mechanics, Chinese Academy of Sciences, Beijing 100190, PR China

ARTICLE INFO

ABSTRACT

In the present research, a systematical study of trans-scale mechanics theory is performed. The surface/interface energy density varying with material deformation is considered, and the general surface/interface elastic constitutive equations are derived. New methods to determine the material length scale parameter and the surface elastic parameters based on a simple quasi-continuum method, i.e. the Cauchy–Born rule, are developed and applied to typical fcc metals. In the present research, the material length parameters will be determined through an equivalent condition of the strain energy density calculated by adopting the strain gradient theory and by adopting the Cauchy–Born rule, respectively. Based on the surface constitutive equations obtained in the present research, the surface elastic parameters are calculated by using the Gibbs definition of surface energy density and the Cauchy–Born rule method.

© 2014 Académie des sciences. Published by Elsevier Masson SAS. All rights reserved.

1. Introduction

Differing from conventional material, modern material in overall or in local is precisely designed and manufactured starting from its microstructure. This is a major feature for modern material. Therefore, modern materials often display good mechanical properties. It is expectable that with wide applications of modern materials, quality and life of products should be improved greatly. However, mechanical behavior of modern materials is microstructure sensitive, and generally speaking conventional mechanics theories cannot characterize the mechanical behavior of modern materials effectively, so that an effective mechanics theory is needed, which can describe the above-mentioned trans-scale mechanics behavior.

Previously, one investigated the above problems mainly from two independent ways: one of them was to present the strain gradient theories for describing the strain gradient effects caused by the material microstructure formation and evolution; the other one was to develop the surface/interface theories for describing the surface/interface effects due to nanostructure deformation and evolution around the surface or interface.

It is well known that there exist many researches on both strain gradient theories and surface/interface effects. In the present introduction, we intend to give a brief review of the types of size-effect study methods, and gradually introduce the trans-scale mechanics theory and the parameter identification problem, instead of providing with mass literatures.

Size effect of the mechanical behavior of microstructured material can be interpreted effectively by adopting strain gradient theories, in which through considering the contributions of the higher-order stresses and strain gradients, the material-inherent scales are introduced and the size effect of mechanical behavior of microstructured materials can be

---

* Corresponding author.
  E-mail address: Ywei@LNM.imech.ac.cn (Y. Wei).

characterized [1]. Until now, the research work on the strain gradient theories has been performing [1–6]. Previously, the length scale parameters included in the strain gradient theories were measured mainly through simulating experimental results of small-size specimens [7,8]. Some investigators studied the mechanical behavior size effect for microstructured materials by considering micro-polar effect [9]. When material cell size is at the nanometer scale, since the specific surface area (SSA) is so high to reach the order of $(10^6–10^9)$/m [10], the magnitude of surface/interface energy is high to be comparable to that of the strain energy, and surface/interface theories considering the surface/interface effects were presented for describing the size effect of the mechanical behavior [10–13]. However, the size effects characterized by the surface/interface theories happen only within a very small scale (below 10 nanometers). Until now, the research work on the surface/interface effects has been performing [14–20].

Summarizing previous researches on the size effects, only considering the strain gradient effect the mechanical behavior of nanostructured materials, cannot be described effectively, while merely considering the surface/interface effect the mechanical behavior of microstructured materials is not described well. Therefore, we presented a trans-scale mechanics theory by which both strain gradient effect and the surface/interface effect are considered simultaneously, and we built up an overall frame of the theory and made the theory applied to the analysis of grain size effect of the nanocrystalline materials [21]. In a previous version of trans-scale mechanics theory, the surface/interface energy density was taken as a material parameter unchanged with deformation.

From materials physics, the surface/interface effect is the state difference between atoms situated at the surface/interface and those located within the material's interior. Different states of atoms bring different energies, depending on atom location—on the surface/interface or at the material interior—, which influences the overall mechanical behavior of materials. In studying the surface/interface effect, a most fundamental concept is the surface/interface free energy. There have been many researches on the surface/interface energy. A definition of surface energy was presented by Gibbs [22]. Surface energy describes the surplus energy of surface atoms relative to the interior atoms. Currently, there are three kinds of approaches for determining surface energy, which are experimental measurement, theoretical modeling, and numerical simulation [23]. Surface stress is also an important quantity to describe the solid surface behavior [22]. Differing from liquid surface, solid surface will cause the surface stress. Shuttleworth defined the surface stress as a differential of surface energy to surface strain [24]. Surface stress has a considerable influence on the nanostructured material behavior [25].

There have been many researches on the surface stress and surface constitutive relation. Maede and Vanderbilt [26] and Needs [27] studied the surface stresses of semiconductor element and metal element by using *ab initio* calculations. Shenoy [28] studied the surface constitutive relation and derived the surface elastic constants, and he obtained the formulas of the surface elastic parameters. Mi et al. [29] and Pahlevani and Shodja [30] investigated the surface stress and the surface elastic parameters through molecular dynamics (MD) simulation.

In the present research, a systematical study on the trans-scale mechanics theory is performed. The surface/interface energy density varying with the material's deformation is considered, and general surface/interface elastic constitutive equations are derived. New methods for determining the material length scale parameter and the surface elastic parameters based on a simple quasi-continuum method, the Cauchy–Born rule (CBR), are developed and applied to typical fcc metals.

Determination of material length parameters is different from conventional methods that simulate experimental results of small-size specimens. In the present research, the material's length parameters will be determined through an equivalent condition of the strain energy density calculated by adopting the strain gradient theory and by adopting the CBR, respectively.

In the determination method of surface elastic parameters, firstly, based on the surface constitutive equations obtained in the present research, the relations of surface elastic parameters with surface energy density are derived; secondly, surface elastic parameters are calculated by using Gibbs' definition of surface energy density and the CBR method.

2. Trans-scale mechanics theory

2.1. Variation equations of the total potential for solids

In conventional theory, the total potential for solids is:

$$\int_V \boldsymbol{\sigma} \delta \boldsymbol{\varepsilon} \, dV - \int_V \bar{\mathbf{f}} \delta \mathbf{u} \, dV - \int_S \bar{\mathbf{t}} \delta \mathbf{u} \, dS = 0 \tag{1}$$

where $(\boldsymbol{\sigma}, \boldsymbol{\varepsilon}, \mathbf{u}, \bar{\mathbf{t}}, \bar{\mathbf{f}})$ are the tensor or vector of stress, strain, displacement, traction and volume force.

For trans-scale mechanics theory, considering both strain gradient effect and surface/interface effect, the variation equation of the total potential can be expressed as follows [21]:

$$\int_V (\boldsymbol{\sigma} \delta \boldsymbol{\varepsilon} + \boldsymbol{\tau} \delta \boldsymbol{\eta}) \, dV + \delta \int_{S'} \gamma \, dS' - \int_V \bar{\mathbf{f}} \delta \mathbf{u} \, dV - \int_S \left(\bar{\mathbf{t}} \delta \mathbf{u} + \bar{\mathbf{S}}_0^{\,s} \delta \boldsymbol{\varepsilon}^s + \bar{\mathbf{r}} \cdot (\delta \mathbf{u} \mathbf{n} \cdot \nabla) \right) dS = 0 \tag{2}$$

where $\boldsymbol{\tau}$ and $\boldsymbol{\eta}$ are the tensors of higher-order stress and strain gradient, $\boldsymbol{\tau} \delta \boldsymbol{\eta}$ is the variation of strain energy density contributed from strain gradient effect, $\bar{\mathbf{r}} \cdot (\delta \mathbf{u} \mathbf{n} \cdot \nabla)$ is the surface-specific work done by higher-order stress moment, γ is

surface/interface energy density, $\delta \int_{S'} \gamma \, dS'$ is the variation of surface/interface energy calculated along the transient surface area, $\bar{\mathbf{S}}_0{}^s \delta \boldsymbol{\varepsilon}^s$ is surface/interface residual work.

In Eq. (2), we considered the small strain case. Specifically, for surface energy, its total contribution comes from two parts: one part is from surface energy density, another part is from surface area variation. The surface energy density is composed of two parts, one part is residual energy density and another part comes from surface strain. Therefore, for small strain case, the calculation of total surface energy should be based on the present domain instead of the reference domain.

If the representative cell size of solid is at the micrometer scale, the surface/interface effect is small and can be neglected relative to the strain gradient effect; however, when it is at the nanometer scale, the surface/interface effect is important and cannot be neglected compared to strain gradient effect.

2.2. Characterizations of strain gradient effect and material length scale

Taking the representative cell size of the solid as the micrometer scale, the surface/interface effect is small and can be neglected relative to the strain gradient effect, and the variation equation of trans-scale mechanics theory (Eq. (2)) will be degenerated into the variation equation of the strain gradient theory as follows [2]:

$$\int_V (\boldsymbol{\sigma}\,\delta\boldsymbol{\varepsilon} + \boldsymbol{\tau}\,\delta\boldsymbol{\eta})\,dV - \int_V \bar{\mathbf{f}}\delta\mathbf{u}\,dV - \int_S \left(\bar{\mathbf{t}}\delta\mathbf{u} + \bar{\mathbf{r}} \cdot (\delta\mathbf{u}\mathbf{n} \cdot \nabla)\right)dS = 0 \tag{3}$$

The simplification form of the comparable strain gradient elasticity for $l^{(k)} = l$ ($k = 1, 4$) can be written as [2,3]:

$$\sigma_{ij} = 2\mu\varepsilon_{ij} + \lambda\varepsilon_{kk}\delta_{ij}, \qquad \tau_{ijk} = 2El^2\eta_{ijk}, \quad \eta_{ijk} = \frac{\partial^2 u_k}{\partial x_i \partial x_j} \tag{4}$$

where l is material length scale, and $\mu = E/(1+\nu)$, $\lambda = E\nu/(1-2\nu)(1+\nu)$ are Lame constants of material, E and ν are Young's modulus and Poisson's ratio.

Young's modulus and Poisson ratio can be measured frequently through mechanical property experiments, while material length scale parameter was previously determined through making a match between experimental results for small-size specimens and simulation results based on the strain gradient theory.

In the present research, a new method is developed to determine the material length-scale parameter. Through energy equivalency based on the strain gradient theory and on the CBR, the material length scale parameter is determined. (See Section 3.)

Expressions of the strain energy density and of its volume average value along the representative cell are given as follows when strain gradient effect is considered:

$$w_{SG} = \frac{1}{2}(\sigma_{ij}\varepsilon_{ij} + \tau_{ijk}\eta_{ijk}), \qquad \bar{w}_{SG} = \frac{1}{V}\int_V w_{SG}\,dV \tag{5}$$

The equivalent theorem to determine the length-scale parameter can be expressed as:

$$\bar{w}_{CB} = \bar{w}_{SG} \tag{6}$$

where $\bar{w}_{CB}$ is the average value of the strain energy density based on the CBR (see Section 3.2). One can obtain the material length scale parameter l appearing in the strain gradient theory expressed by the microscopic physics parameters.

2.3. Characterizations of surface/interface effect and constitutive equations

In the present research, differing from previous methods (by definitions), we used a very simple method, energy variational method, to derive out the surface/interface theory, which is same as the commonly used Shuttleworth's version of the surface/interface theory [24,28].

Based on the variation of surface energy, $\delta \int_{S'} \gamma \, dS'$ (referring to Eq. (2)), further derivations are performed. The sketch figures of surface area after and before deformation (S' and S) are shown in Fig. 1, where S is the surface area in its initial configuration, corresponding to surface coordinates X_1, X_2. Undergoing a deformation gradient $\mathbf{F}$, surface area after deformation is S', corresponding to surface coordinates x_1, x_2 at transient configuration. According to deformation geometry, one has:

$$x_i = F_{ij}X_j \tag{7}$$

The definition of surface Green's strain is:

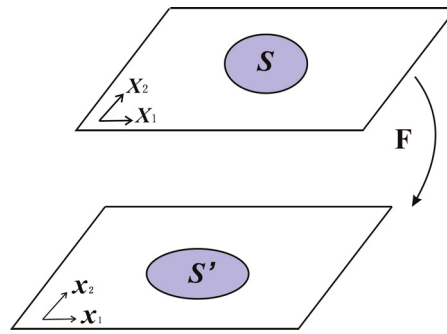$$\varepsilon^s{}_{ij} = \frac{1}{2}(F_{ki}F_{kj} - \delta_{ij}) \tag{8}$$

Fig. 1. Sketch of surface area before and after deformation.

where δ_{ij} is the Kronecker symbol. The relation between S and S' can be expressed as:

$$S' = S \det \mathbf{F} = S J^s = S \sqrt{\det(\mathbf{I} + 2\boldsymbol{\varepsilon}^s)} \tag{9}$$

So we have:

$$\delta \int_{S'} \gamma \, \mathrm{d}S' = \int_S \delta(\gamma J^s) \, \mathrm{d}S = \int_S \left[J^s \frac{\partial \gamma}{\partial \boldsymbol{\varepsilon}^s} \delta \boldsymbol{\varepsilon}^s + \gamma \frac{\partial J^s}{\partial \boldsymbol{\varepsilon}^s} \delta \boldsymbol{\varepsilon}^s \right] \mathrm{d}S$$

$$= \int_S J^s \left[\mathbf{f}^s + \gamma \left[(\mathbf{I} + 2\boldsymbol{\varepsilon}^s)^{-1} \right] \right] \delta \boldsymbol{\varepsilon}^s \, \mathrm{d}S = \int_{S'} \left[\mathbf{f}^s + \gamma \left[(\mathbf{I} + 2\boldsymbol{\varepsilon}^s)^{-1} \right] \right] \delta \boldsymbol{\varepsilon}^s \, \mathrm{d}S' \tag{10}$$

where

$$\mathbf{f}^s = \partial \gamma / \partial \boldsymbol{\varepsilon}^s, \qquad \partial J^s / \partial \boldsymbol{\varepsilon}^s = J^s \left[(\mathbf{I} + 2\boldsymbol{\varepsilon}^s)^{-1} \right] \tag{11}$$

If surface constitutive relations are introduced, the variation of surface energy can be expressed by surface stress and surface strain as follows:

$$\delta \int_{S'} \gamma \, \mathrm{d}S' = \int_{S'} \mathbf{S}^s \delta \boldsymbol{\varepsilon}^s \, \mathrm{d}S' \tag{12}$$

So the surface stress can be expressed as:

$$\mathbf{S}^s = \frac{\partial \gamma}{\partial \boldsymbol{\varepsilon}^s} + \gamma \left[(\mathbf{I} + 2\boldsymbol{\varepsilon}^s)^{-1} \right] \tag{13}$$

When surface strain tends to zero, one can obtain the formulas of surface residual stress:

$$\overline{\mathbf{S}^s} = \frac{\partial \gamma}{\partial \boldsymbol{\varepsilon}^s} \bigg|_{\boldsymbol{\varepsilon}^s = 0} + \gamma \mathbf{I} \tag{14}$$

Linear elastic relation of surface constitutive equation between surface stress and surface strain is given as:

$$\mathbf{S}^s = \overline{\mathbf{S}^s} + \mathbf{D}^s \boldsymbol{\varepsilon}^s \tag{15}$$

So the surface elastic coefficient $\mathbf{D}^s$ can be expressed as:

$$\mathbf{D}^s = \frac{\partial \mathbf{S}^s}{\partial \boldsymbol{\varepsilon}^s} \tag{16}$$

$\mathbf{D}^s$ is a fourth-order tensor; its components can be expressed as follows:

$$D^s{}_{ijkl} = \frac{\partial S^s{}_{ij}}{\partial \varepsilon^s{}_{kl}} \bigg|_{\boldsymbol{\varepsilon}^s = 0} = \left(-2\gamma \delta_{ik} \delta_{jl} + \delta_{ij} \frac{\partial \gamma}{\partial \varepsilon^s{}_{kl}} + \frac{\partial^2 \gamma}{\partial \varepsilon^s{}_{ij} \partial \varepsilon^s{}_{kl}} \right) \bigg|_{\boldsymbol{\varepsilon}^s = 0} \tag{17}$$

where $i, j, k, l = 1, 2$.

From Eqs. (10)–(17), it is worth noting that the surface/interface energy depends only on the classical strain, and the effect of the curvature of the surface is neglected. It is related to the definition of the surface/interface constitutive relation. If the constitutive relation is defined as the high-order relation, the surface/interface energy will depend on both classical strain and high order strain, and the effect of the surface curvature will be considered. In the present research, for simplicity, we focus our attention on the low-order surface/interface constitutive relation.

3. Material length scale characterization

3.1. Solution based on strain gradient elasticity for spherical expanding model

In order to determine the material length scale parameter value, we use a spherical expanding cell model. It is noting that there exists the exact solution for Wei–Hutchinson's strain gradient theory. The representative cell size of the spherical model can be reached at the micrometer scale, so the surface/interface effect is small and can be neglected relative to the strain gradient effect.

The strain energy density for the spherical expanding model based on the strain gradient theory can be given by (referring to [31]):

$$w_{SG} = \frac{1}{2}\left\{ (\lambda + 2\mu)u'^2 + 4\lambda\left(\frac{u \cdot u'}{r}\right) + 4(\lambda + \mu)\left(\frac{u}{r}\right)^2 + 2El^2\left[u''^2 + 6\left(\frac{u'}{r} - \frac{u}{r^2}\right)^2\right]\right\} \tag{18}$$

where radial displacement is:

$$u(r) = Ar + \frac{B}{r^2}\left[(r - L)e^{\frac{r}{L}} + (r + L)e^{-\frac{r}{L}}\right], \quad L = l\sqrt{2E/(\lambda + 2\mu)} \tag{19}$$

where r is the radial coordinate; unknown constants A and B can be determined by the outer boundary conditions for the spherical expanding model:

$$u(r)|_{r=R} = (\lambda_1 - 1)R + \frac{3}{2a}\lambda_2 R^2$$

$$\left.\frac{du(r)}{dr}\right|_{r=R} = \lambda_1 - 1 + 3\lambda_2 \cdot \frac{R}{a} \tag{20}$$

where R is spherical radius, λ_1 stands for a uniform expanding ratio, expanding gradient on the outer boundary is described by the term $3\lambda_2 R/a$ where a is a reference length and is taken as the atomic lattice size in the present research. λ_2 describes the spherical expanding gradient.

Using Eqs. (19) and (20), A and B can be given as follows:

$$A = \lambda_1 - 1 + \frac{3\lambda_2 R}{2a} - \frac{3\lambda_2 R[(R - L)e^{R/L} + (R + L)e^{-R/L}]}{2a[(R^2/L + 3L - 3R)e^{R/L} - (R^2/L + 3L + 3R)e^{-R/L}]}$$

$$B = \frac{3\lambda_2 R^4}{2a[(R^2/L + 3L - 3R)e^{R/L} - (R^2/L + 3L + 3R)e^{-R/L}]} \tag{21}$$

3.2. Solution based on the CBR for the spherical expanding model

By the CBR, the relation of relative atomic distances before and after deformation is assumed as [32]:

$$\boldsymbol{r}_{ij} = \boldsymbol{F} \cdot \boldsymbol{R}_{ij} \tag{22}$$

where $\boldsymbol{r}_{ij}$ and $\boldsymbol{R}_{ij}$ are the relative atomic distances (atom i and atom j) after and before deformation, respectively, $\boldsymbol{F}$ is the deformation gradient corresponding to a continuum deformation and is a tensor field function. By the CBR, a discrete system moving is treated with a continuum body deformation.

The second-order CBR was also developed for describing a non-uniform deformation problem [33,36]. The fundamental relation can be read as:

$$\boldsymbol{r}_{ij} = \boldsymbol{F} \cdot \boldsymbol{R}_{ij} + \frac{1}{2}\boldsymbol{G} : [\boldsymbol{R}_{ij} \otimes \boldsymbol{R}_{ij}]$$

$$\boldsymbol{G} = \nabla\boldsymbol{F} \tag{23}$$

The interaction between atoms is governed through potential, such as the Lennard-Jones (L-J) pair potential,

$$\varphi(r_{ij}) = 4e\left[\left(\frac{r_0}{r_{ij}}\right)^{12} - \left(\frac{r_0}{r_{ij}}\right)^6\right] \tag{24}$$

in which two atoms i and j are at the relative distance $\boldsymbol{r}_{ij}$. The parameters e and r_0 represent the energy at the minimum in $\varphi(r_{ij})$ and the distance to zero.

It is worth noting that for the spherical expanding model, there exists a quickly convergent solution of strain energy based on the pair-potential for the Cauchy–Born rule; it just can be matched with the exact solution based on the strain gradient theory. This is the reason why we adopted the pair-potential here.

Table 1
The related microscopic physics parameters and macroscopic mechanical parameters for typical fcc metals adopted in the present research.

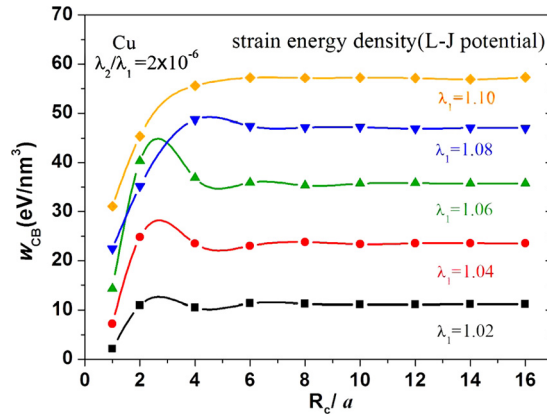| Metals (fcc)	Young's modulus (GPa)	Poisson ratio	Lattice size a (Å)	L–J potential parameter σ (Å)	L–J potential parameter ε (eV)
Cu	119	0.33	3.61	2.28	0.42
Al	70	0.35	4.05	2.55	0.41
Ni	200	0.32	3.52	2.22	0.53
Ag	83	0.33	4.09	2.57	0.35
Au	79	0.42	4.08	2.57	0.46
Pt	170	0.40	3.92	2.47	0.69
Pd	121	0.39	3.89	2.45	0.47

Fig. 2. Relations of the average strain energy density with spherical radius.

Restricted to classical lattice static, the energy contribution E_i of atom i to potential energy can be expressed as:

$$E_i = \frac{1}{2} \sum_{j \neq i} \varphi(r_{ij}) = \frac{1}{2} \sum_{j \neq i} \varphi\big(|\mathbf{r}_{ij}|\big) \tag{25}$$

Then we can derive out the average strain energy density:

$$\bar{w}_{\text{CB}} = \frac{\Delta E_i(\mathbf{F}; \mathbf{G}; \mathbf{R}_{ij})}{V_i} = \frac{1}{2V_i} \sum_{j \neq i} \big[\varphi\big(|\mathbf{r}_{ij}|\big) - \varphi\big(|\mathbf{R}_{ij}|\big)\big] \tag{26}$$

where V_i denotes the effective volume around the atom i, and can be expressed as:

$$V_i = \frac{V}{N} \tag{27}$$

where V is the total volume of the body (sphere), N is the total numbers of the atoms in the spherical body.

In the present research, we adopt the second-order CBR for the gradient expanding problem of the spherical body, so non-zero components of the deformation gradient and its higher-order gradient are given as (referring to Eq. (20)):

$$F_{rr} = \lambda_1 + \lambda_2 \cdot \frac{R_{ij}}{a}, \qquad G_{rrr} = \frac{\lambda_2}{a} \tag{28}$$

where $R_{ij} = |\mathbf{R}_{ij}|$, a is the atom lattice size.

Based on the second order CBR, the average value of the strain energy density can be calculated by using Eqs. (23), (24), (26), and (28). The material length scale parameter can be expressed by some microscopic physics parameters through using the equivalent condition of average strain energy density, Eq. (6).

3.3. Results and discussions

During the present calculations, the related microscopic physics parameters for typical fcc metals were taken from the literatures, and listed in Table 1.

In order to examine the effect of spherical radius in spherical expanding model, the relations of the average strain energy density with spherical radius are calculated and the results are shown in Fig. 2 for fcc metal Cu. From Fig. 2, fortunately, the average strain energy density are independent of the spherical radius when the radius is larger than about 8 times the
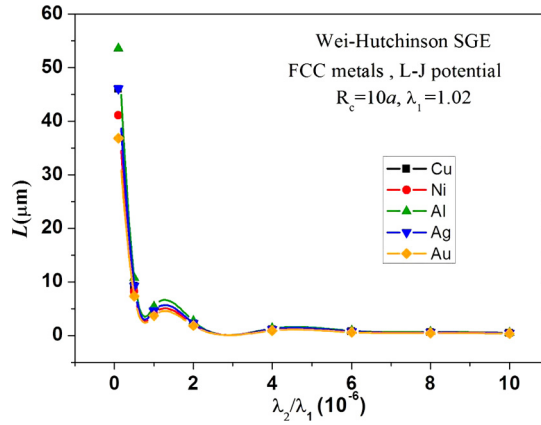
Fig. 3. Relations of the composite length scale with the normalized expanding gradient for several typical fcc metals.
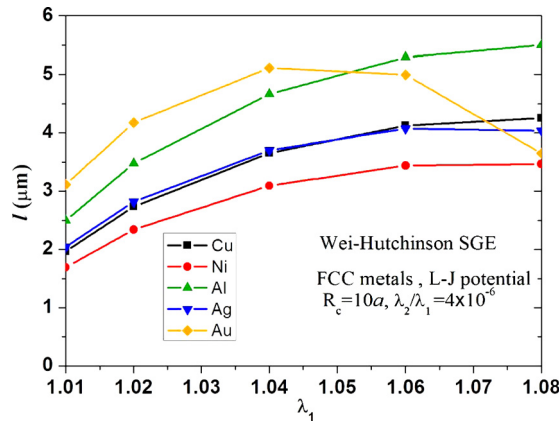

Fig. 4. Length scale parameters for several typical fcc metals calculated through the equivalent theorem of strain energy density.

atom lattice size for different spherical expanding ratios. Therefore, in the present research, spherical radius in the spherical expanding model is taken as 10 times the atom lattice size.

In order to examine the effect of the spherical expanding gradient, the relations of the composite length scale L (Eq. (19)) with normalized expanding gradient are calculated for several typical fcc metals, as shown in Fig. 3. From Fig. 3, when value of the normalized expanding gradient λ_2/λ_1 is larger than 2×10^{-6}, the results tend to be stable. Therefore, in the present analysis, we take the value of the normalized expanding gradient as 4×10^{-6}.

Through the equivalent theorem of average strain energy density, the material length scale parameters for several typical fcc metals are calculated. The relations of the materials' length scale parameters with spherical expanding ratio are given in Fig. 4. From Fig. 4, within the typical value scope of the spherical expanding ratio (1.01, 1.08), the length scale parameters for several typical fcc metals are taken in the scope of (1.7, 5.5) microns, which is consistent with those given by measuring and simulating the small-size specimens [7,8]. From Fig. 4, one can find $l_{Al} > l_{(Cu,Ag)} > l_{Ni}$.

From Figs. 3 and 4, the result of the length scale parameter at the micrometer scale weakly depends on the boundary conditions described by two parameters ($1.0 < \lambda_1 < 1.1$ and $2\lambda_1 \times 10^{-6} < \lambda_2 < \lambda_1 \times 10^{-5}$). However, the stress and strain results should closely depend on the boundary conditions because two parameters describe the external strain exerting on the external boundary.

4. Surface elastic parameter characterization

4.1. Calculation of surface energy density

The definition of surface energy given by Gibbs was adopted [22]. Due to the difference of status of surface atoms with interior atoms, there is a difference between the energies brought by these two kind of atoms. Comparing with interior atom, the surplus energy in surface atoms is called surface free energy. Through comparing total energy in nanoplate with

that corresponding to the interior atoms with identical numbers, the difference of energy is the surface free energy. Surface energy density can be expressed as:

$$\gamma = \frac{\sum_{i=1}^{n} E_i - n E_b}{2A} \tag{29}$$

where n is the atom number in the nanoplate, E_i is the energy of the ith atom, E_b is the energy of the interior atom, A is the surface area of the nanoplate.

In the present research, a calculation model is selected, with a thickness that is 5 times the lattice size; inside the surface, each side is 30 times the lattice size and periodic boundary conditions are applied, and relaxation is considered for the outer surface only.

4.2. Surface stress and surface elastic coefficients

In the present research, our analyses are applied to fcc metals along (100) and (111) surfaces. There is only one non-zero independent component of surface stress, i.e. $\overline{S^s_{11}} = \overline{S^s_{22}}$, $\overline{S^s_{12}} = 0$; thus surface stress of fcc metal can be further expressed as:

$$\overline{S^s_{11}} = \left(\gamma + \frac{\partial \gamma}{\partial \varepsilon^s_{11}} \right)_{\boldsymbol{\varepsilon}^s = 0} \tag{30}$$

There are three independent non-zero surface elastic parameters, $D^s_{1111} = D^s_{2222}$, $D^s_{1122} = D^s_{2211}$ and D^s_{1212} [28]. Their expressions can be written as follows:

$$D^s_{1111} = \left(-2\gamma + \frac{\partial \gamma}{\partial \varepsilon^s_{11}} + \frac{\partial^2 \gamma}{\partial \varepsilon^s_{11}{}^2} \right)\Bigg|_{\boldsymbol{\varepsilon}^s = 0} \tag{31}$$

$$D^s_{1212} = \left(-2\gamma + \frac{\partial^2 \gamma}{\partial \varepsilon^s_{12}{}^2} \right)\Bigg|_{\boldsymbol{\varepsilon}^s = 0} \tag{32}$$

$$D^s_{1122} = \left(\frac{\partial \gamma}{\partial \varepsilon^s_{22}} + \frac{\partial^2 \gamma}{\partial \varepsilon^s_{11} \partial \varepsilon^s_{22}} \right)\Bigg|_{\boldsymbol{\varepsilon}^s = 0} \tag{33}$$

Generally, surface energy density γ is a function of surface strain $\boldsymbol{\varepsilon}^s$. For a simple deformation case (one dimensional strain), γ can be expanded a series of ε,

$$\gamma = \gamma^0 + A_1 \varepsilon + A_2 \varepsilon^2 + A_3 \varepsilon^3 + \cdots \tag{34}$$

For example, $\overline{S^s_{11}}$, D^s_{1111}, D^s_{1212} are related with the surface strain component only, corresponding to uniaxial tension/compression and pure shear, respectively. Through different deformation cases, one can obtain the γ value and its relation with surface strain; furthermore, surface elastic parameters can be obtained. However, for D^s_{1122}, two components of surface strain are concerned; a double axial deformation model (double axial tension/compression) is considered in the present research. A polynomial expression of γ is used as:

$$\gamma = \gamma^0 + B_1 \varepsilon_{11} + B_2 \varepsilon_{22} + B_3 \varepsilon_{11} \varepsilon_{22} + B_4 \varepsilon_{11}^2 + B_5 \varepsilon_{22}^2 + \cdots \tag{35}$$

During calculation, the determination of coefficients B_i is made through selecting the ratio of $\varepsilon_{11}/\varepsilon_{22}$ in double axial tension/compression, and thus D^s_{1122} is determined. The above-mentioned uniaxial tension/compression, pure shear and double axial tension/compression can be described by the CBR [30] for the proper potentials. Corresponding deformation gradients can be given as follows:

$$\mathbf{F}_1 = \begin{bmatrix} 1 + \varepsilon_{11} & \\ & 1 \end{bmatrix} \tag{36}$$

$$\mathbf{F}_2 = \begin{bmatrix} 1 & \varepsilon_{12} \\ & 1 \end{bmatrix} \tag{37}$$

$$\mathbf{F}_3 = \begin{bmatrix} 1 + \varepsilon_{11} & \\ & 1 + \varepsilon_{22} \end{bmatrix} \tag{38}$$

4.3. Johnson's potential

In the present research, the Johnson potential (embedded atom potential) [34] is used to describe the surface/interface mechanical behavior. Johnson potential can be read as:
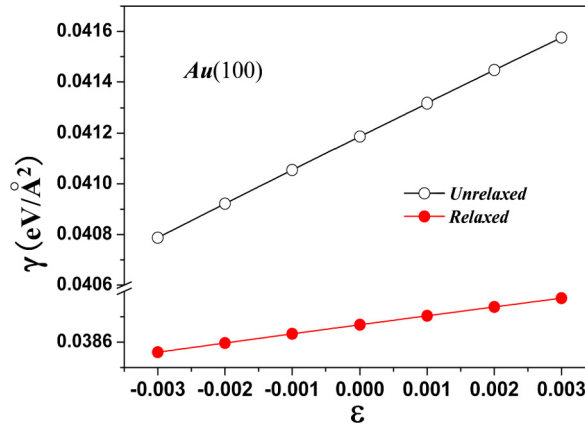
Fig. 5. Relations of surface energy density of Au (100) with strain.

Table 2
Surface elastic parameters of the (100) free surface calculated for fcc metals using the Johnson EAM potential (the first row); the next row represents the corresponding results extracted from [29]. Units: eV/Å².

Fcc	γ		$\overline{S^s}_{11}$		D^s_{1111}		D^s_{1212}		D^s_{1122}	
	U	R	U	R	U	R	U	R	U	R
Au	0.054	0.051	0.222	0.089	−1.326	−0.510	−0.387	−0.301	−0.703	−0.402
	0.054	0.051	0.220	0.093	−1.192	−0.443	−0.282	−0.198	−0.758	−0.354
Cu	0.078	0.078	0.105	0.068	−0.628	−0.418	−0.224	−0.232	−0.005	−0.122
	0.077	0.076	0.118	0.088	−0.557	−0.395	−0.079	−0.084	−0.070	−0.036
Pd	0.090	0.090	0.203	0.090	−1.467	−0.726	−0.360	−0.349	−0.703	−0.643
	0.087	0.086	0.212	0.124	−1.310	−0.757	−0.188	−0.177	−0.720	−0.481
Pt	0.096	0.093	0.320	0.146	−2.022	−0.917	−0.590	−0.501	−1.163	−0.861
	0.097	0.092	0.322	0.157	−1.835	−0.827	−0.403	−0.320	−1.054	−0.581

$$E_t = \sum_i F(\rho_i) + \frac{1}{2} \sum_i \sum_{j, j \neq i} \varphi(r_{ij}) \quad \rho_i = \sum_{j, j \neq i} f(r_{ij})$$

$$f(r) = f_e \exp\left[-\beta(r/r_e - 1)\right]$$

$$\varphi(r) = \varphi_e \exp\left[-\gamma(r/r_e - 1)\right]$$

$$F(\rho) = -E_c(1 - \ln x)x - 6\varphi_e y$$

$$x = (\rho/\rho_e)^{\alpha/\beta} \qquad y = (\rho/\rho_e)^{\gamma/\beta} \tag{39}$$

where coefficients $f_e, \varphi_e, E_c, \alpha, \beta, \gamma$ are given in [29], ρ_e is the electronic density when the atom is at equilibrium state. Here we adopted the embedded atom potential for surface parameter identification in order to compare the present result with MD simulation results based on the same potential in literatures.

4.4. Results and discussions

In order to investigate the influence of atom relaxation on the results, we calculate the relation of surface energy density with strain under uniaxial tension for Au (100) adopting Sutton potential [35]. The result is shown in Fig. 5. From Fig. 5, surface energy density increases monotonically with the applied strain. The relation can be well simulated by using a quadratic function.

When once the relation of surface energy density with applied strain is obtained, surface stress and surface elastic parameters can be calculated by using Eqs. (30)–(33). Surface elastic parameters calculated for typical fcc metals are given in Tables 2 and 3. In these tables, the results based on both unrelaxed configuration ("U") and relaxed configuration ("R") are shown. Johnson potential is used, and the corresponding results are compared with others results based on the MD simulation [29].

In tables, results shown in the first row are the present results based on the CBR, while the results shown in the second row represent the corresponding results based on the molecular dynamics calculation extracted from [29]. Adopting Johnson potential, we calculate Au, Cu, Pd and Pt. Comparing the results shown in Tables 2–3, one can find that the results based on the CBR are consistent with other results adopting the MD calculations, and this was explained as a simple quasi-continuum

Table 3

Surface elastic parameters of the (111) free surface calculated for fcc metals using the Johnson EAM potential (the first row); the next row represents the corresponding results extracted from [29]. Units: eV/Å^2.

Fcc	γ		$\overline{S^s}_{11}$		D^s_{1111}		D^s_{1212}		D^s_{1122}	
	U	R	U	R	U	R	U	R	U	R
Au	0.046	0.045	0.195	0.149	−1.031	−0.808	−0.260	−0.228	0.083	−0.906
	0.046	0.044	0.193	0.104	−0.918	−0.509	−0.392	−0.192	−0.166	−0.106
Cu	0.072	0.072	0.067	0.057	−0.212	−0.182	−0.214	−0.210	−1.44	−0.196
	0.071	0.070	0.079	0.059	−0.155	−0.100	0.075	0.093	−0.076	−0.066
Pd	0.081	0.080	0.167	0.127	−1.020	−0.827	−0.295	−0.275	−0.144	−0.970
	0.078	0.077	0.174	0.115	−0.878	−0.614	−0.432	−0.286	−0.135	−0.105
Pt	0.084	0.083	0.275	0.211	−1.463	−1.162	−0.417	−0.375	0.814	0.661
	0.084	0.081	0.275	0.165	−1.297	−0.803	−0.521	−0.283	−0.250	−0.177

method; the CBR is an effective method to characterize the solid surface elastic behavior. With regard to the consistency of two kind of results based on both CBR and MD, the calculated surface energy densities have a best consistency than the calculated surface stresses, and there is little difference for the calculated surface elastic parameters.

In the present research, the CBR is used to describe atomic moves by which the atomic moving orbit is determined by a deformation gradient of an imaginary continuum structure, so that the calculation quantity decreases considerably compared to that adopting MD calculation. Through the above comparison of the results of both method, we evidence once again that as a simple quasi-continuum method, CBR, may be a reliable method to describe the mechanical behavior of nanostructured materials.

With regard to the relaxation effect, through comparing the results shown in Table 2 and Table 3, one can find that the effects of relaxation on the surface energy density are not obvious; however, if effects on the surface stress and the surface elastic parameters are obvious, it is because that surface stress and surface elastic parameters include derivatives of surface energy density, so they are more obviously depending on the initial configuration. From Tables 2 and 3, surface stress is positive, while surface elastic parameters are often negative. For fcc metals, the surface energy density on (111) is smaller than that on (100).

It is worth noting that there exists a big difference about partial results of D^s_{1122} on (111) with other results based on the MD calculation; the reason may be that for a surface with dense atom arrangement, atom moving is too complicated to be described by using the simple CBR method.

5. Conclusions

In the present research, we have investigated the trans-scale mechanics theory, systematically, and a complete theoretical description has been performed. The determination methods of the material length scale parameter and of the surface elastic parameters have been presented, in which the material length scale parameter is determined by using an energy equivalent method that let strain energy density based on the strain gradient theory equal to that based on the CBR. Simultaneously, for the research of surface effect based on the CBR, new methods for determining the surface energy density and surface elastic parameters have been developed. With regard to the surface effect research, firstly, based on the variation of surface energy, we have derived and given the definitions of the surface stress and surface elastic parameters. Secondly, adopting the CBR and the atom interaction potential, Johnson's embedded atom potential, we have characterized the nanoplate configuration of typical fcc metals and obtained the relation of surface energy density with strain. Thirdly, based on the relation of surface energy density with strain, we have calculated the surface stress and surface elastic parameters for typical fcc metals, which are consistent with other results based on the MD calculations, and we have evidenced that the simple CBR method is effective to describe surface elastic parameters.

Acknowledgements

References

[1] N.A. Fleck, J.W. Hutchinson, Strain gradient plasticity, in: J.W. Hutchinson, T.Y. Wu (Eds.), Adv. Appl. Mech., vol. 33, Academic Press, New York, 1997, pp. 295–361.

[2] Y.G. Wei, A new finite element method for strain gradient theories and applications to fracture analyses, Eur. J. Mech. A, Solids 25 (2006) 897–913.

[3] Y.G. Wei, J.W. Hutchinson, Steady-state crack growth and work of fracture for solids characterized by strain gradient plasticity, J. Mech. Phys. Solids 45 (1997) 1253–1273.

[4] Y.G. Wei, Particulate size effects in the particle-reinforced metal-matrix composites, Acta Mech. Sin. 17 (2001) 45–58.

[5] S. Forest, N.M. Cordero, E.P. Busso, First vs. second gradient of strain theory for capillarity effects in an elastic fluid at small length scales, Comput. Mater. Sci. 50 (2011) 1299–1304.

[6] K.A. Lazopoulos, A.K. Lazopoulos, On the torsion problem of strain gradient elastic bars, Mech. Res. Commun. 45 (2012) 42–47.

[7] J.S. Stolken, A.G. Evans, A microbend test method for measuring the plasticity length scale, Acta Mater. 46 (1998) 5109–5115.

[8] M.R. Begley, J.W. Hutchinson, The mechanics of size-dependent indentation, J. Mech. Phys. Solids 46 (1998) 2049–2068.

[9] Hansong Ma, Gengkai Hu, Eshelby tensors for an ellipsoidal inclusion in a micropolar material, Int. J. Eng. Sci. 44 (2006) 595–605.

[10] X.L. Chen, H.S. Ma, L.H. Liang, Y.G. Wei, A surface energy model and application to mechanical behavior analysis of single crystals at sub-micron scale, Comput. Mater. Sci. 46 (2009) 723–727.

[11] H.L. Duan, J. Wang, B.L. Karihaloo, Z.P. Huang, Nanoporous materials can be made stiffer than non-porous counterparts by surface modification, Acta Mater. 54 (2006) 2983–2990.

[12] W. Gao, S.W. Yu, G.Y. Huang, Finite element characterization of the size-dependent mechanical behavior in nanosystems, Nanotechnology 17 (2006) 1118–1122.

[13] Gang-Feng Wang, Xi-Qiao Feng, Tie-Jun Wang, et al., Surface effects on the near-tip stresses for mode-I and mode-III cracks, J. Appl. Mech. 75 (2008) 011001.

[14] M.E. Gurtin, A. Ian Murdoch, A continuum theory of elastic material surfaces, Arch. Ration. Mech. Anal. 57 (4) (1975) 291–323.

[15] D.J. Steigmann, R.W. Ogden, Elastic surface–substrate interactions, Proc. R. Soc. A 455 (1982) (1999) 437–474.

[16] R. Dingreville, J. Qu, Surface free energy and its effect on the elastic behavior of nano-sized particles, wires and films, J. Mech. Phys. Solids 53 (8) (2005) 1827–1854.

[17] A. Javili, P. Steinmann, On thermomechanical solids with boundary structures, Int. J. Solids Struct. 47 (24) (2010) 3245–3253.

[18] B. Bar On, E. Altus, E.B. Tadmor, Surface effects in non-uniform nanobeams: continuum vs. atomistic modeling, Int. J. Solids Struct. 47 (9) (2010) 1243–1252.

[19] J. Yvonnet, A. Mitrushchenkov, G. Chambaud, Q.C. He, Finite element model of ionic nanowires with size-dependent mechanical properties determined by ab initio calculations, Comput. Methods Appl. Mech. Eng. 200 (5–8) (2011) 614–625.

[20] D. Davydov, A. Javili, P. Steinmann, On molecular statics and surface-enhanced continuum modeling of nano-structures, Comput. Mater. Sci. 69 (0) (2013) 510–519.

[21] B. Wu, L.H. Liang, H.S. Ma, Y.G. Wei, A trans-scale model for size effects and intergranular fracture in nanocrystalline and ultra-fine polycrystalline metals, Comput. Mater. Sci. 57 (2012) 2–7.

[22] J.W. Gibbs, The Collected Works of J. Willard Gibbs, vol. I, Thermodynamics, Longmans, Green, and Company, New York, 1928.

[23] Baoqin Fu, Analysis and Calculation of Surface Energy with the Empirical Electron Theory in Solid and Molecule[D], Beijing University of Chemical Technology, China, 2010.

[24] R. Shuttleworth, The surface tension of solids, Proc. Phys. Soc. A 63 (1950) 444–457.

[25] H.S. Park, Quantifying the size-dependent effect of the residual surface stress on the resonant frequencies of silicon nanowires if finite deformation kinematics are considered, Nanotechnology 20 (2009) 206102.

[26] R.D. Meade, D. Vanderbilt, Origins of stress on elemental and chemisorbed semiconductor surfaces, Phys. Rev. Lett. 63 (1989) 1404.

[27] R.J. Needs, Calculations of the surface stress tensor at aluminum (111) and (110) surface, Phys. Rev. Lett. 58 (1987) 53–56.

[28] Vijay B. Shenoy, Atomistic calculations of elastic properties of metallic fcc crystal surfaces, Phys. Rev. B 71 (2005) 094104.

[29] Changwen Mi, Sukky Jun, D.A. Kouris, Atomistic calculations of interface elastic properties in noncoherent metallic bilayers, Phys. Rev. B 77 (2008) 075425.

[30] Ladan Pahlevani, Hossein M. Shodja, Surface and interface effects on torsion of eccentrically two-phase fcc circular nanorods: determination of the surface/interface elastic properties via an atomistic approach, J. Appl. Mech. 78 (2011) 011011.

[31] X.L. Gao, S.K. Park, H.M. Ma, Analytical solution for a pressurized thick-walled spherical shell based on a simplified strain gradient elasticity theory, Math. Mech. Solids 14 (8) (2009) 747–758.

[32] M. Born, K. Huang, Dynamical Theory of Crystal Lattices, Oxford University Press, Oxford, UK, 1954.

[33] R. Sunyk, P. Steinmann, On higher gradients in continuum-atomistic modeling, Int. J. Solids Struct. 40 (24) (2003) 6877–6896.

[34] R.A. Johnson, Alloy models with the embedded-atom method, Phys. Rev. B 37 (1989) 12554.

[35] H. Rafii-Tabar, A.P. Sulton, Long-range Finnis–Sinclair potentials for fcc metallic alloys, Philos. Mag. Lett. 63 (1991) 217–224.

[36] P. Steinmann, A. Elizondo, R. Sunyk, Studies of validity of the Cauchy–Born rule by direct comparison of continuum and atomistic modeling, Model. Simul. Mater. Sci. Eng. 15 (2007) S271–S281.